Research Article

Effect of Incorporating TiO₂ Photocatalyst in PVDF Hollow Fibre Membrane for Photo-Assisted Degradation of Methylene Blue

Norashima Abdullah[a], Bamidele V. Ayodele[a,b], Wan Nurdiyana Wan Mansor[c], Sureena Abdullah[a,b]*

[a]Faculty of Chemical & Natural Resources Engineering, Universiti Malaysia Pahang, Malaysia
[b]Center of Excellence for Advanced Research in Fluid Flow, Lebuhraya Tun Razak, 26300 Gambang Kuantan, Pahang, Malaysia
[c]School of Ocean Engineering, Universiti Malaysia Terengganu, KualaNerus, 21030 Terengganu, Malaysia

Abstract

A rapid growth in populations, living standards and industries has become a key contribution to water pollution. Clean water is an important resource for life, sustainable development and ecosystems. This study therefore investigates the photocatalytic degradation of an organic pollutant (methylene blue) using PVDF/TiO₂ membrane. The main objective of the study is to determine the synergistic effect of incorporating TiO₂ photocatalyst into the PVDF membrane on the mineralization of the organic pollutants. The TiO₂ photocatalyst was characterized using Ultraviolet Visible Spectroscopy (UV-Vis), Scanning Electron Microscopy (SEM), Brunauer, Emmettt, and Teller (BET), and X-ray Diffraction (XRD) techniques. While the fabricated PVDF/TiO₂ hollow fibre membranes were then characterized by scanning electron microscopy (SEM) and contact angle. The performance of the membrane was evaluated by photodegradation of methylene blue. The degradation study revealed that both the undoped PVDF and the TIO₂ doped PVDF membrane were capable of degrading methylene blue. The performance of the membrane can be ranked as follows 9 wt% TiO₂/PVDF > 6 wt% TiO₂/PVDF > 3 wt% TiO₂/PVDF > undoped PVDF showing the synergistic effect of incorporating the TiO₂ photocatalyst into the PVDF membrane. The kinetics data of obtained from the rate of degradation of the methylene blue fitted well into first order kinetic data with apparent kinetic constants of 0.0591, 0.0295, 0.0188, and 0.0100 obtained using pure membrane, undoped PVDF, 3 wt% TiO₂/PVDF, 6 wt% TiO₂/PVDF, and 9 wt% TiO₂/PVDF, respectively.

Keywords: Water pollution; titanium dioxide; photocatalytic degradation; methylene blue; polyvinylidene fluoride

1. Introduction

Having a high-water quality is an important criterion in achieving a sustainable life [1]. Often time, industrial effluents containing organic pollutants are being discharged into water bodies without proper treatment [2]. Report had shown that a large fraction of the total world production of dyes usually find its way into the textile effluents during dyeing process [3]. These organic pollutants which contain highly carcinogenic and mutagenic compounds and not properly treated could result in distortion of ecological balance in the water bodies and pose serious health risk to both human and aquatic lives [4]. One of such organic pollutant is methylene blue which is a deep-coloured organic

* Corresponding Author.
  E-mail: sureena@ump.edu.my (S. Abdullah)

compound that has wide application in the dying and textiles processes [5]. In the past years, research efforts have geared towards developing effective techniques to remove and degrade these organic pollutants from water effluent discharged from the textile industries [4]. The conventional techniques, such as: adsorption, sedimentation, and coagulation, have been investigated however being replaced with more advanced techniques, such as: advanced oxidation processes [6]. Advanced oxidation processes (AOPs) have received an increasing attention for water and wastewater treatment [7]. AOPs differ from conventional physical and biological processes as they generate a strong oxidant which is hydroxyl radicals to degrade toxic and refractory pollutants into simple and harmless inorganic molecules without generating secondary waste [8]. The most attractive feature of AOPs is that its highly potent and strongly oxidizing radical that allows the destruction of a wide range of organic chemical substrate with no selectivity [1].

Advanced oxidation process, such as: photolysis, Fenton method, photofenton, ozonolysis, sonolysis, and photocatalysis, have been widely investigated with each methods having its merits and demerits [9,10]. Besides AOPs techniques for wastewater treatment, membrane filtration has also been proven as an effective means of wastewater treatment due to its compactness, ease of fabrication, operation and module design [11]. Nevertheless, the technique is constraint by membrane fouling which often results in the shortening of the membrane life [12]. One way to mitigate the constraint of membrane fouling and improve the performance of the membrane filtration is by modification of the membrane surface with an inorganic nanoparticle, such as: TiO_2. One major advantages of the TiO_2 photocatalyst is its potential anti fouling activities [11]. Besides, the TiO_2 being a photocatalyst will enhance the waste water treatment process by combining membrane filtration and photodegrading. Photocatalysis being one of the most versatile advanced oxidation processes has the merit of utilizing the abundant source of ultraviolent (UV) radiation from sunlight in the presence of a photocatalysts usually a semiconductor, such as: TiO_2. One of the merits of photocatalysis is its possibility of generating powerful reactive hydroxyl radicals with photon energy without require additional chemicals [13].

Over these years, several semiconductors such as Fe-$ZnIn_2S_4$ [14], WO_3 [15-16], BiOBr [17], Bi_3O_4Br and $BiFeO_3$ [18], Fe_2O_3 [19,20],

CuS [21], $Bi_{24}O_{31}Br_{10}$ [22], and ZnO [16], have been explored as photocatalysts. Among those, titanium dioxide (TiO_2) has attracted public concern as a promising photocatalyst due to the fact that it is inexpensive, commercially available, nontoxic and chemically stable [23-27]. The performance of photocatalysis can be enhanced by incorporating the chemical process together with membrane separation process often referred to as photocatalytic membrane. The use of photocatalytic membrane process has become increasingly important due to advantages such as high productivity and selectivity, compact and small size equipment, lower cost and energy consumption [28-30].

The presence study therefore aimed to harness the synergy of incorporating membrane to photocatalytic process for the photo-degradation of methylene blue. In this work, the synergetic effect of incorporating TiO_2 photocatalysts into polyvinylidene fluoride (PVDF) membrane for the photo-degradation of methylene blue under UV irradiation was investigated.

2. Materials and Method

2.1 Materials

The organic pollutant, methylene blue, the N,N-dimethylacetamide (DMAc), and 99.9% of ethanol were purchased from Merck and used as received. The P-25 titanium dioxide (TiO_2) was also purchased from Merck and used as a photocatalyst. The PVDF polymer was utilized as membrane due to its chemical stability and resistance to solvents, acids, bases and heat. The solution containing the methylene blue was prepared using de-ionized water obtained from our research laboratory.

2.2 Methods

2.2.1 Fabrication of the PVDF/TiO_2 membrane

To prepare the PVDF/TIO_2 membrane, TiO_2 was dissolved in the N,N-dimethylacetamide solvent. After the mixture dissolved, the desired amount of polymer (PVDF) was added to the solution and stirred at 70-80 °C for 12 h. Afterward, the mixture was cooled down to room temperature. The detailed composition of the PVDF and the doped TiO_2 in the solutions and spinning conditions are shown in Table 1. The solution was degassed at ambient temperature overnight prior to spinning. The dope solution was then extruded using a spinneret to form hollow fibre membrane. The as-spun hollow fibres were immersed into water bath for 3

days to remove residual solvent. The fibres were post-treated using (ethanol: water, 50:50 wt%) for 1 h, then 100% of ethanol for 1 h in order to improve the membrane wettability and pore collapse. Finally, the hollow fibre membranes were dried at room temperature for 3 days before membrane characterizations and module fabrication.

2.3 Characterization of the PVDF/TiO$_2$ Membrane

The properties of TiO$_2$ photocatalyst in terms of the band gap, surface area and crystallinity were determined using ultraviolet visible (UV-Vis) spectroscopy, Brunauer, Emmett, and Teller (BET), and X-ray diffraction (XRD) techniques, respectively. The UV-visible spectrum was measured at room temperature using Perkin Elmer/Lambda 1050 UV/Vis/NIR spectrophotometer to determine the band gap of the catalyst. To define the band gap, an amount catalyst, powdered titanium dioxide (TiO$_2$) was taken and placed in sample holder. It was then compressed into a thin layer and put into ultra violet visible machine. The sample was run in 200 to 600 nm range of wavelength.

Meanwhile, the XRD analysis of the membrane was subsequently analyzed using a Panalytic Al X'pert diffractometer system at 2θ. The Panalytic Al X'pert diffractometer system is equipped with Cu rotating anode capable of generating voltage and tube current of 40 V and 40 mA respectively. The BET analysis was measured using Micrometrics BET surface area and porosity analyzer (Micrometrics ASAP 2020). The sample was initially degassed at 250 ℃ for 3 h. Liquid N$_2$ at -196 ℃ was gradually adsorbed on the TiO$_2$ sample. The specific surface area of the TiO$_2$ was measured using BET method.

On the other hand, the morphology of the membrane was characterized by scanning electron microscopy (SEM). In order to measure the morphology of the PVDF/TiO$_2$ membrane, the hollow fibre membrane was immersed in liquid nitrogen for five minutes and then fractured into short samples for the purpose of maintaining the original cross sectional of the membranes. The samples were positioned on stubs for measurement. The micrographs of the cross section of hollow fibre membranes were taken at different magnifications using SEM (Model: Hitachi/TM 3030, Plus, Japan).

Contact angle measurement is crucial in determining the hydrophobicity or hydrophilicity surfaces of the membrane. The static contact angle of the outer surface of hollow fibre membranes were measured using a contact angle goniometer. The hollow fibre membrane samples were fixed on a slide glass before the contact liquid was dropped (2 µL) by micro syringe. The surface angle was measured at several different spots on each membrane sample. Finally, the values were averaged and used for standard deviation calculation.

2.4 Photocatalytic Degradation Activity

The photocatalytic degradation of the methylene blue was performed in a photoreactor system. Prior to the experiment, a module which consist of 16 bundles of the TiO$_2$/PVDF hollow membrane was sealed into a PVC tube with the aid of epoxy resin. Afterwards, the module was allowed to harden at room temperature before cutting the protruding parts which was subsequently fixed into a PVC adapter. Subsequently, the as-prepared module was fitted into the ultraviolet photoreactor system (1 Liter capacity) which consist of a rectangular glass tank. The feed solution is made up of 400 mL of methylene blue solution with an initial concentration of 1 mol/L.

The methylene blue solution was agitated for about 20 min without light source in order

Table 1. The dope compositions and spinning conditions of hollow fibre membrane.

Conditions	Values			
Dope composition (wt%)		PVDF	TiO$_2$	DMAc
	Sample A	15	0	85
	Sample B	15	3	82
	Sample C	15	6	79
	Sample D	15	9	76
Bore fluid composition	80% deionized water/ 20% DMAc			
Bore fluid flowrate	1.5 min/s			
Spinneret dimension OD/ID	1.0 mm/0.5 mm			

to attain equilibrium adsorption on the surface of the TiO_2/PVDF prior to the photodegradation test. Thereafter, the methylene blue solution was irradiated with UV light sourced from 175 W high pressure mercury lamp at irradiance of 100 mW/cm². The UV lamp was placed above the methylene blue solution at a distance of 10 cm. At interval of 30 min irradiation time, a sample of the solution was taken, centrifuged and filtered. The residual concentration of the methylene blue from the sample was measured using UV-vis spectrophotometer at 664 nm (maximum absorption for methylene)

3. Results and Discussion

3.1 XRD Analysis

The XRD analysis examines the crystalline nature of TiO_2 photocatalyst which is depicted in Figure 1. TiO_2 exists in three different forms namely rutile, anatase and brookite [31]. Luttrell et al. [31] revealed that the photocatalytic activity of TiO_2 in anatase form is much higher than the other forms. It can be seen from Figure 1 that the three primary peaks exists at 25.5°, 37.9°, and 48.2º which can be assigned to diffraction at (101), (004), and (200) plane of anatase respectively. The XRD analysis shows that the TiO_2 photocatalyst is mainly in the form of anatase which is consistent with join committee on powder diffraction standards (JCPDS card, 21-1272) [32]. The crystallite size of the TiO_2 was estimated using Scherrer formula (Equation (1)) as 39.58 nm.

$$D = \frac{K\lambda}{\beta \cos \theta} \tag{1}$$

where, D is the crystallite size, λ is the wavelength of X-ray radiation (CuK_α radiation, λ=

0.15418), β is the line width at medium height, and θ is the diffraction peak angle.

3.2 UV-Vis Spectrophotometric Analysis

The band gap energy of the TiO_2 was investigated under ultraviolet visible (UV-Vis) spectroscopy as depicted in Figure 2. Band gap energy (E) refers to the energy difference between conduction band and valence band of the catalyst [33]. The band gap energy is an important parameter for a photocatalytic reaction to occur using a photocatalyst. The band gap and the particle size are dependent on each. Hence, a small particle has a wide band gap. The display of wide band gap by small particle could be as result of the fewer molecular orbitals being added to the possible energy states of the particles [33]. The cut off wavelength was found at 410 nm. The band gap energy of the TiO_2 was calculated using Equation (2) as 3.03 eV.

$$E = \frac{hc}{\lambda} \tag{2}$$

where, E is the band gap energy, h is the Planck's constant (6.626×10^{-34} J.s), c is the speed of light (3.0×10^8 m/s), and λ is the cut off wavelength.

The diffuse reflectance spectra of the un-doped PVDF membrane and the TiO_2 doped PVDF membrane measured at different time interval ranging from 0 min to 90 min are depicted in Figure 3. The absorption range of the pure membrane as well as the TiO_2 doped PVDF membrane were observed from 400 nm to 800 nm and found to correspond to UV absorption characteristic of PVDF membrane and TiO_2-doped PVDF membrane. It can be seen that the TiO_2 doping on the membrane slightly
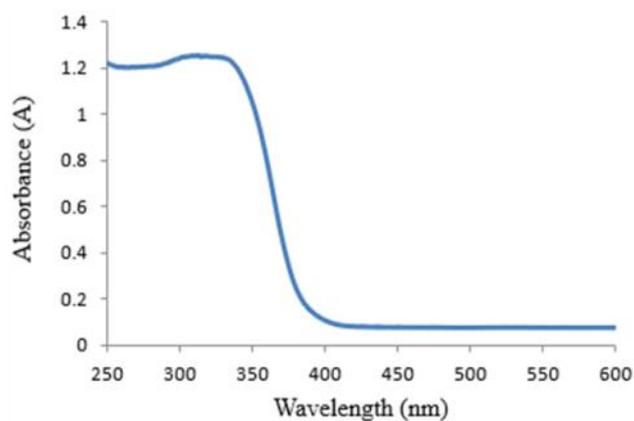

Figure 1. XRD pattern of anatase TiO_2

Figure 2. The absorbance of TiO_2 photocatalyst

affect the absorption properties of the PVDF membranes as shown in the UV-Vis spectra.

3.3 Surface Area

The N_2 adsorption-desorption isotherm of the TiO_2 photocatalyst is depicted in Figure 4. According to the IUPAC system, the isotherm plot was categorized as Type V which implies the weak adsorbate-adsorbate interactions which is typical characteristic of porous adsorbents. Figure 5 represent the surface area plot and the value has been estimated using the BET and found to be 10.11 m^2g^{-1}, which revealed the potential of TiO_2 as a good photocatalytic candidate.

3.5 SEM Analysis

The morphology of the PVDF membrane showing the cross section of the inner and outer structure obtained from the SEM analysis is depicted in Figure 5. According to Damodar et al. [34], the hydrophilicity characteristic of a membrane depends on how well the catalyst disperse over the membrane. Generally, a typical membrane consists of two distinct layers compose of sponge and finger like layer where the later one was formed underneath of the former one. It can be seen from the SEM images the formation of a finger-like structure from the outer to intermediate layer of the membrane while the rest was the formation of sponge-like structure. The thickness of the finger-like structure for the undoped PVDF in Figure 5(a) was 69.0 µm. With doping of 3 wt% of the TiO_2 catalyst, the thickness of the finger-like structure increases to 72.3 µm (Figure 5(b)). This could be attributed to the dispersion of TiO_2 on the PVDF thereby creating room for the methylene blue molecules to penetrate the outer layer of the membrane for degradation [35]. The increase in the finger-like
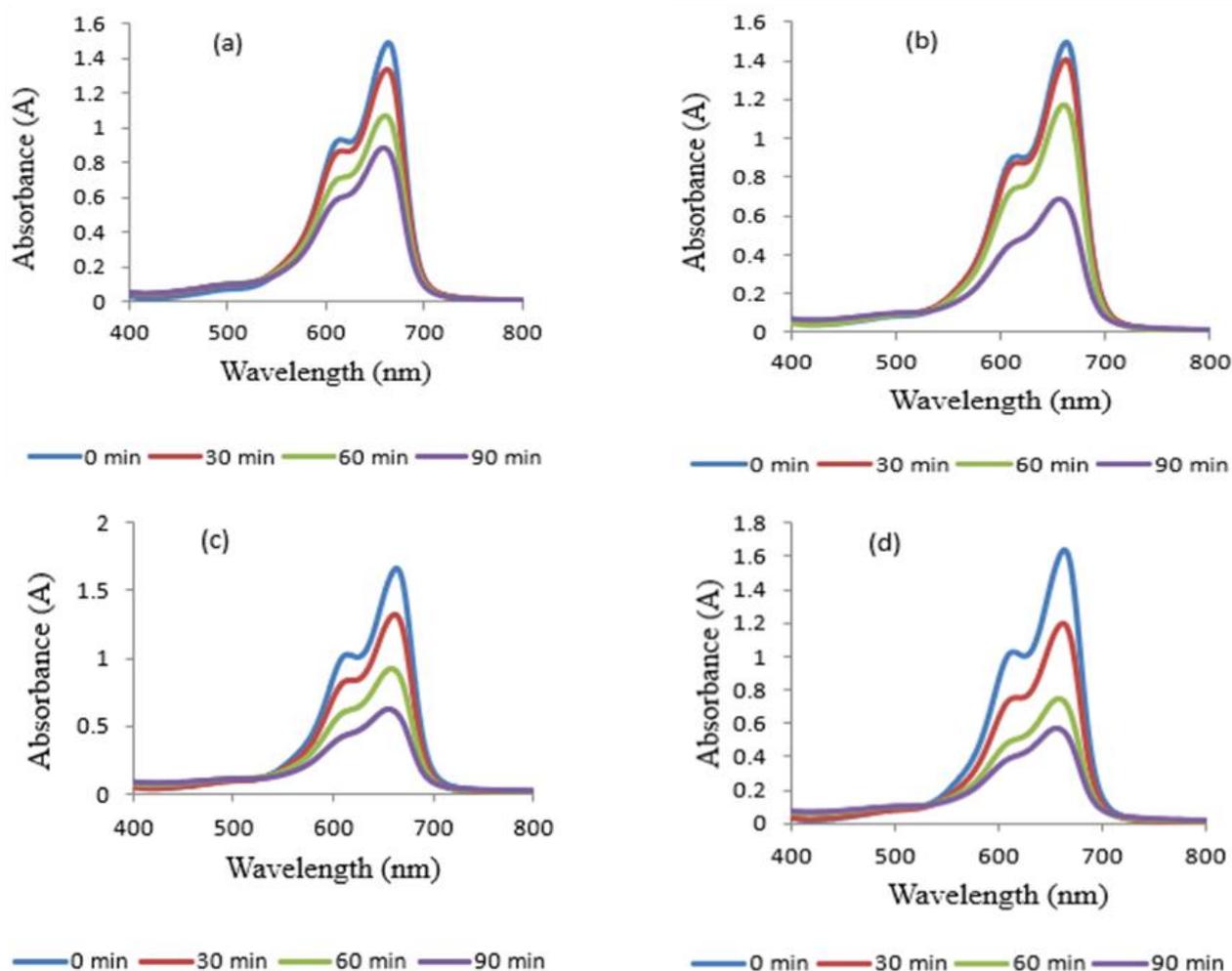

Figure 3. The diffuse reflectance spectra of (a) undoped PVDF (b) 3 wt% TiO_2/PVDF (c) 6 wt% TiO_2/PVDF and (d) 9 wt% TiO_2/PVDF

structure could be attributed to increase in the TiO_2 loading which could provide more surface area that could accelerate the rate of photocatalytic degradation [35]. The weak interaction of the polymer-solvent and additive could be responsible for the elongation of the finger-like structure. Hence, it can be implied that the membrane structure is affected by the concentration of the additive.

3.6 Contact Angle Analysis

Surface hydrophilicity plays an important role in the characteristics of photocatalytic-based membrane due to its crucial effect on the flux and antifouling properties [36]. This reason could be attributed to the presence of the rich hydroxyl-group in TiO_2 with high affinity for water molecules on the membrane surface [37]. The different values of the contact angles for undoped PVDF and PVDF with varying TiO_2 loadings are summarized in Table 2. Although, PVDF is well known as hydrophobic, it can be seen that the tendency of PVDF to own hydrophilicity characteristics is increases as the TiO_2 was added.

The initial contact angle of PVDF membrane was measured to be 91.60° which indi-

cates the intrinsic and superior hydrophobicity of PVDF membrane. The contact angle 91.60° also implies an intensive electronegative characteristics of fluorine element resulting in the low surface energy of fluoropolymers and weak affinity of PVDF toward water [38-39]. It can be seen that the mean values of the contact angles decrease from 91.60° to 42.67° as the doping with the TiO_2 increases. This trend revealed that the hydrophilicity of the PVDF membrane is significantly improved by the incorporation of TiO_2 into the macropores of the PVDF membrane. The improvement in the hydrophilicity of the membrane with increase in TiO_2 doping could be ascribed to the introduction of hydroxyl to the original hydrophobic PVDF membrane.

3.7 The Photodegradation of Methylene Blue

Figure 6 shows the decolourization of the methylene blue via photocatalytic degradation using the undoped PVDF membrane and the various TiO_2 doped PVDF membrane. It is interesting to know that complete decolourization of the methylene blue could be achieved within 90 minutes of photocatalytic reaction time. It is noteworthy that the TiO_2 doped PVDF membrane displayed higher rate of decolourization of the methylene blue compared to the undoped PVDF membrane. The percentage decolourization of the undoped PVDF increases from 10 at 30 min to 67 at 90. On the other hand, a higher percentage decolourization of the methylene was reported for the 3-9 wt%TiO_2-PVDF membrane. This observation could be attributed to the synergistic effect of the TiO_2 on the membrane creating a highly porous structure of the membrane which invariable increases the accessibility of the PVDF membrane site for adsorption and photodegradation of the methylene blue. Hence, it can be inferred that the incorporation of the TiO_2 into the PVDF resulted in a dual process of adsorption and photocatalytic degradation of the methylene blue [35]. Moreover, the decolourization of the methylene blue in-
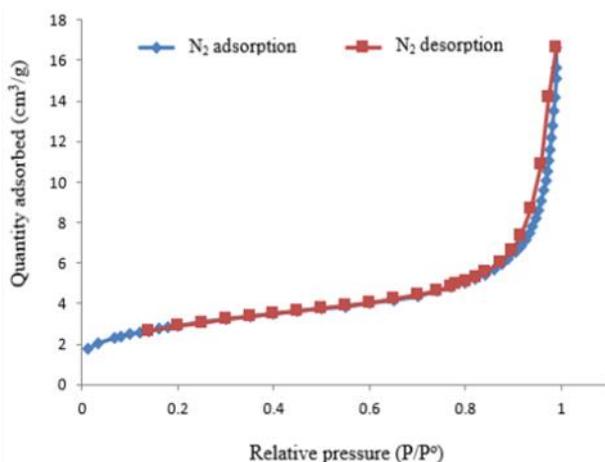

Figure 4. The N_2 adsorption-desorption isotherm of the TiO_2

Table 2. The data tabulations for water contact angle of hollow fibre membranes

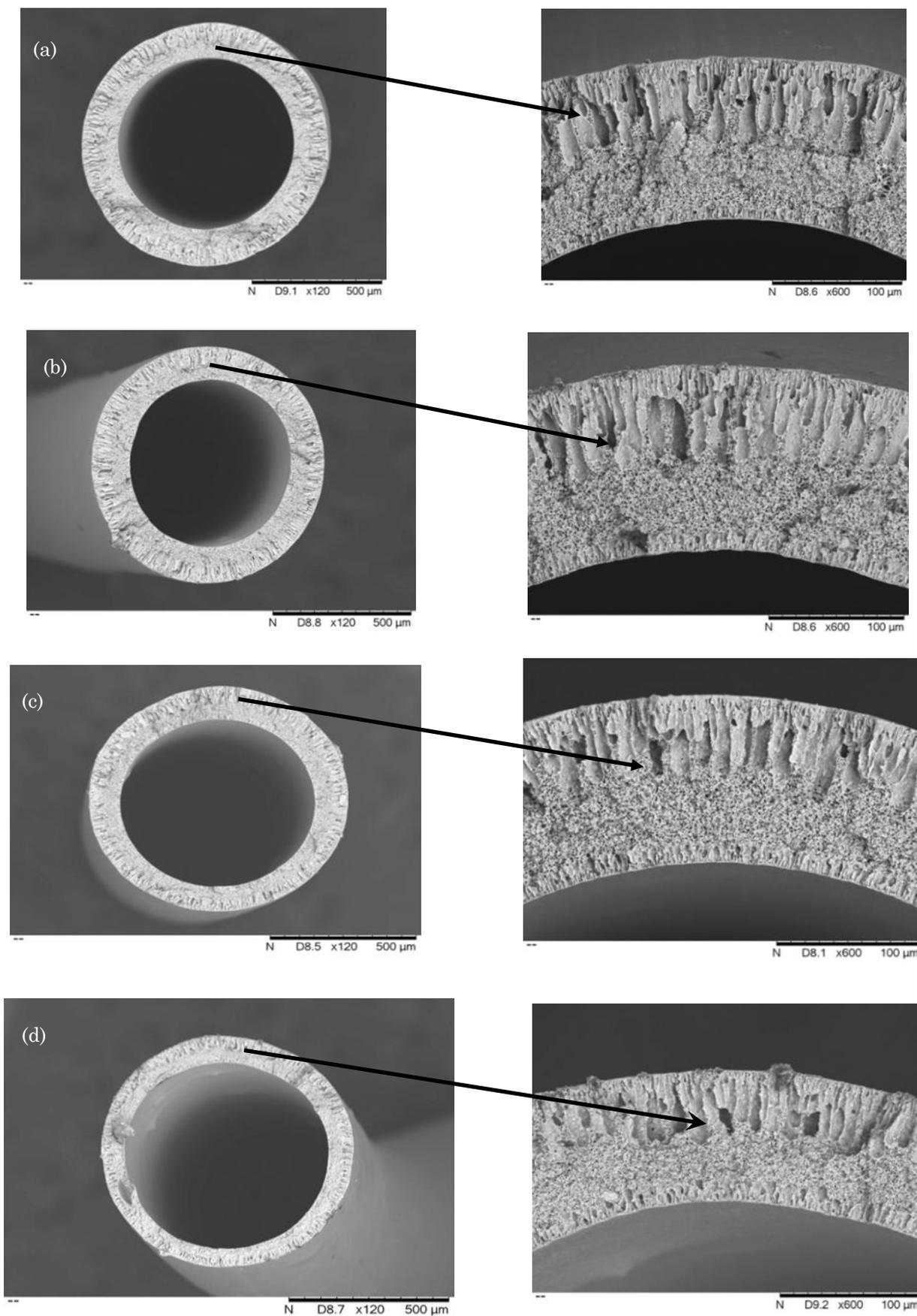| Samples	Contact angle (°)					Mean value (°)
undoped PVDF	93.01	91.05	91.07	91.32	91.49	91.60
PVDF with 3 wt% TiO_2	75.75	73.35	72.32	74.53	74.90	74.19
PVDF with 6 wt% TiO_2	58.72	57.38	56.43	51.03	56.43	56.00
PVDF with 9 wt% TiO_2	43.60	43.00	42.32	42.90	41.54	42.67

Figure 5. The SEM images of (a) undoped PVDF, (b) 3 wt% TiO_2/PVDF, (c) 6 wt% TiO_2/PVDF, and (d) 9 wt% TiO_2/PVDF

creases with the TiO$_2$ doping which implies that the increase in weight of the TiO$_2$ from 3 wt% to 9 wt% provided more catalytic site for the photo-decolourization of the methylene blue. Moreover, according to Ngang et al. [40], the addition of the different weight percentage of the TiO$_2$ also increase the permeability of the PVDF membrane thereby making it more effective for the decolourization of the methylene blue. This observation is also consistent with the work of Houas et al. [41] who employed TiO$_2$ for the photodegradation of methylene blue under UV light. It can be inferred that the decolourization of the methylene blue occurs simultaneously by adsorption using membrane and photocatalytic reaction by the TiO$_2$.

3.8. Kinetic Analysis

The kinetics of photocatalytic degradations of organic inorganic pollutants have been investigated using Langmuir-Hinshelwood expression represented [42]. In this study, it is proposed that the phocatalytic degradation of the methylene blue can be fitted to the Langmuir-Hinshelwood model due to the following reasons: the reaction occur between two adsorbed substance; the reaction take place between a radical in the solution and between and adsorbed substrate molecule; the reaction occurs between a radical linked to the surface and a substrate molecule in solution; the reaction take place with both species being in the solution. The rate expression for the photodegradation of the methylene blue can be represented in Equation (3).

$$r = -\frac{dc}{dt} = \frac{k_r k_a c}{1 + k_a c + k_w c_w + \sum_{i=1}^{n} k_i k_i} \qquad (3)$$

where, r is the reaction for the oxidation of methylene blue, c is the concentration of the methylene blue, k_r is the specific reaction rate for the oxidation of the methylene blue, k_a is the equilibrium adsorption constant of methylene blue, c_w is the concentration of the solvent, k_w is the equilibrium adsorption constant of the solvent, c_i is the concentration of the products, k_i is the equilibrium adsorption constant of the products, and t is the reaction time.

Based on the assumption that there is no competition adsorption between the reactant and the product, $\Sigma_{i=1,n} k_i k_i$ tends to 0. Moreover, $c_w > c$, integrating Equation (3) resulted in Equation (4).

$$ln\left(\frac{c_o}{c}\right) = K't \qquad (4)$$

where, $K' = k_r k_a$ is the apparent first order rate constant. The plot of $ln(c_o/c)$ against t gives a straight line through the origin with K' as the intercept.

Figure 7 depicts the plots of the $ln(c_o/c)$ againt the degradation time for the TiO$_2$-PVDF material. The corresponding apparent rate constants obtained from the plots is summarized in Table 3. Interestingly, it can be seen that the apparent rate constant reduces with increase in the TiO$_2$. The K' values of 0.591, 0.0295, 0.0188, and 0.0100 were obtained for 0 wt% TiO$_2$/PVDF, 3 wt% TiO$_2$/PVDF, 6 wt%
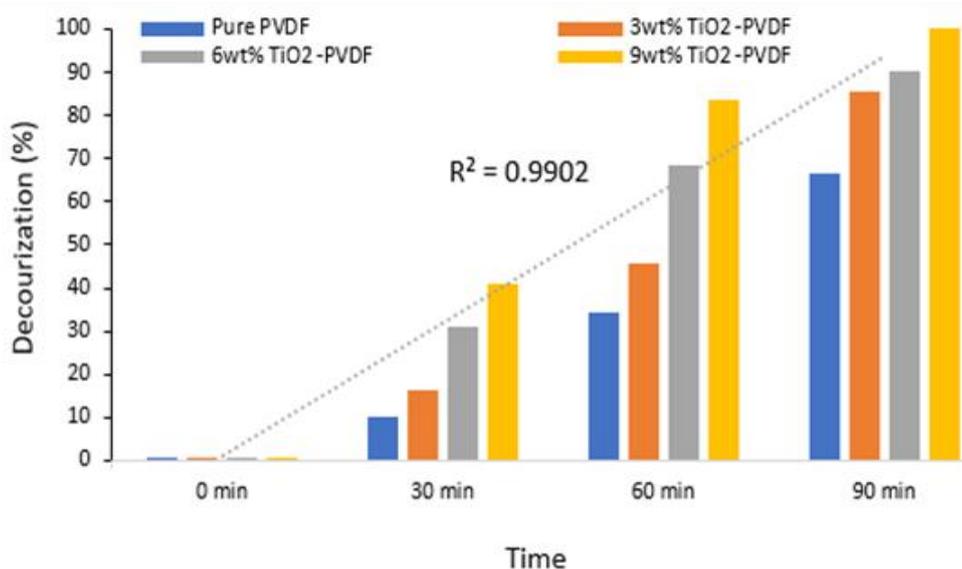

Figure 6. Photocatalytic degradation of methylene blue using different catalyst loadings

TiO$_2$/PVDF, and 9 wt% TiO$_2$/PVDF, respectively. The obtained apparent rate constants is an indication that the doping of the PVDF membrane had significant effect on the rate of degradation of the methylene blue. Hence, the rate of photocatalytic reaction proceeds faster with the increase in the TiO$_2$ loading.

4. Conclusions

The synergistic effect of TiO$_2$ doping on photodegradation of methylene blue using PVDF/TiO$_2$ membrane has been investigated. The PVDF/TiO$_2$ membranes were successfully fabricated and characterized by UV-Vis spectroscopy, N$_2$ physisorption analysis, XRD, SEM, and contact angle in order to have a better understanding on their physicochemical properties. The characterization results showed that the PVDF membrane hydrophilicity were significantly improved by the doping of the different weight percent of the TiO$_2$. The rate of decolourization of the methylene blue during the photocatalytic reaction for 90 minutes can be ranked as 9 wt% TiO$_2$/PVDF, > 6 wt% TiO$_2$/PVDF, > 3 wt% TiO$_2$ /PVDF, > undoped PVDF, an indication of the significant effect of the TiO$_2$ on the photodegradation of the methylene blue. The kinetics data obtained from the rate of degradation of the methylene blue fitted well into first order kinetic data with apparent kinetic constants of 0.0591, 0.0295, 0.0188, and 0.0100 obtained using undoped PVDF membrane, 3 wt% TiO$_2$ /PVDF, 6 wt% TiO$_2$ /PVDF, 9 wt% TiO$_2$ /PVDF membrane, respectively. This study has demonstrated the capability of TiO$_2$/PVDF membrane for the photodegradation of recalcitrant organic pollutant such as methylene blue and could serve as a basis for further work to demonstrate the capabilities of photocatalytic membrane to degrade organic pollutant from industrial effluent in order to obtain clean water for daily use.

Acknowledgment

Table 3. Parameters obtained from the kinetic modeling analysis

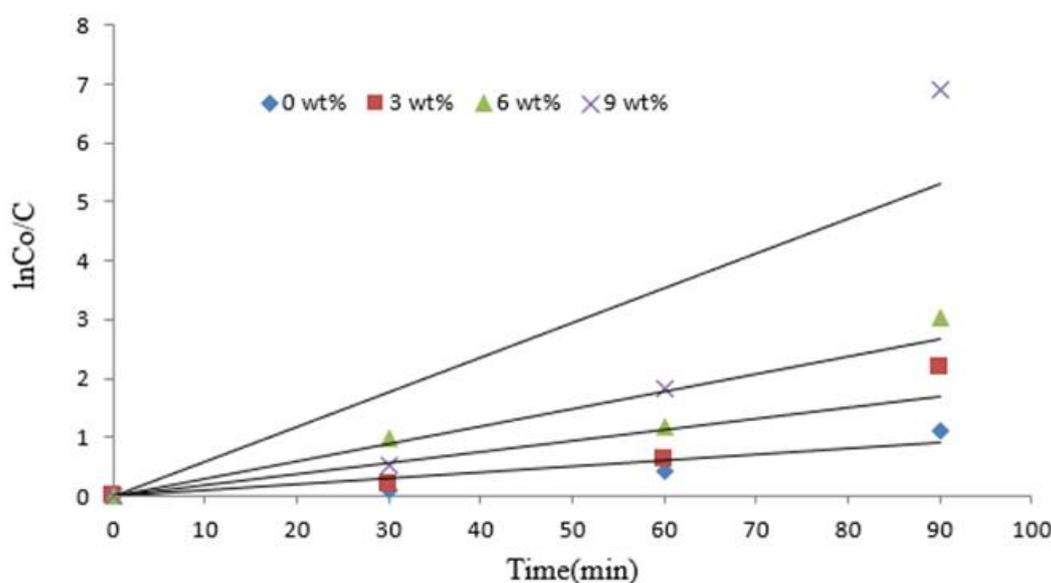| Material	K'	R^2
Undoped PVDF	0.0591	0.763
3wt%TiO2-PVDF	0.0295	0.890
6wt%TiO2-PVDF	0.0188	0.882
9wt%TiO2-PVDF	0.0100	0.846

Figure 7. First order linear plot of the decolourization of methylene blue by photocatalysis under UV irradiation

References

[1] Gaya U.I., Abdullah A.H. (2008). Heterogeneous photocatalytic degradation of organic contaminants over titanium dioxide: A review of fundamentals, progress and problems. *J. Photochem. Photobiol. C Photochem.,* 9 (1):1-12. doi:10.1016/j.jphotochemrev.2007.12.003.

[2] Ebrahiem E.E., Al-Maghrabi M.N., Mobarki A.R. (2017). Removal of organic pollutants from industrial wastewater by applying photo-Fenton oxidation technology. *Arab. J. Chem.* 10:S1674-S1679. doi:10.1016/j.arabjc.2013.06.012.

[3] Zangeneh, H., Zinatizadeh, A.A.L., Habibi, M., Akia, M., Hasnain Isa, M. (2015). Photocatalytic oxidation of organic dyes and pollutants in wastewater using different modified titanium dioxides: A comparative review. *J. Ind. Eng. Chem.* 26:1-36. doi:10.1016/j.jiec.2014.10.043.

[4] Pi, Y., Li, Z., Xu, D., Liu, J., Li, Y., Zhang, F., Zhang, G., Peng, W., Fan, X. (2017). 1T-Phase MoS_2 Nanosheets on TiO_2 Nanorod Arrays: 3D Photoanode with Extraordinary Catalytic Performance. *ACS Sustain. Chem. Eng.*, 5(6): 5175-5182. doi:10.1021/acssuschemeng.7b00518.

[5] Ali, K.A., Abdullah, A.Z., Mohamed, A.R. (2017). Visible light responsive TiO_2 nanoparticles modified using Ce and La for photocatalytic reduction of CO_2: Effect of Ce dopant content. *Appl. Catal. A Gen.*, 537:111–120. doi:10.1016/j.apcata.2017.03.022.

[6] Aksu, Z. (2005). Application of biosorption for the removal of organic pollutants: A review. *Process. Biochem.* 40(3-4): 997-1026. doi:10.1016/j.procbio.2004.04.008.

[7] Oller, I., Malato, S., Sánchez-Pérez, J.A. (2011). Combination of Advanced Oxidation Processes and biological treatments for wastewater decontamination-A review. *Sci. Total Environ.*, 409 (20): 4141-4166. doi:10.1016/j.scitotenv.2010.08.061.

[8] Leong, S., Razmjou, A., Wang, K., Hapgood, K., Zhang, X., Wang, H. (2014). TiO_2 based photocatalytic membranes : A review. *Journal of Membrane Science*, 472: 167-184. doi:10.1016/j.memsci.2014.08.016.

[9] Hidalgo, M.C., Maicu, M., Navío, J.A., Colón, G. (2007). Photocatalytic properties of surface modified platinised TiO_2: Effects of particle size and structural composition. *Catal. Today*, 129 (1-2):43-49. doi:10.1016/j.cattod.2007.06.052.

[10] Malato, S., Blanco, J., Alarcon, D.C., Maldonado, M.I., Fernandez-Ibanez, P., Gernjak, W. (2007). Photocatalytic decontamination and disinfection of water with solar collectors. *Catal. Today,* 122 (1-2): 137-149. doi:10.1016/j.cattod.2007.01.034.

[11] Moghadam, M.T., Lesage, G., Mohammadi, T., Mericq, J.P., Mendret, J., Heran, M., Faur, C., Brosillon, S., Hemmati, M., Naeimpoor, F. (2015). Improved antifouling properties of TiO_2/PVDF nanocomposite membranes in UV-coupled ultrafiltration. *J. Appl. Polym. Sci.* 132 (21):13-15. doi:10.1002/app.41731.

[12] Ochoa, N.A., Masuelli, M., Marchese, J. (2003). Effect of hydrophilicity on fouling of an emulsified oil wastewater with PVDF/PMMA membranes. *J. Memb. Sci.*, 226(1-2): 203-211. doi:10.1016/j.memsci.2003.09.004.

[13] Lin, Z., Zhao L, Dong Y (2015). Chemosphere Quantitative characterization of hydroxyl radical generation in a goethite-catalyzed Fenton-like reaction. *Chemosphere*,141:7–12. doi:10.1016/j.chemosphere.2015.05.066.

[14] Gao, B., Liu, L., Liu, J., Yang, F. (2013). Photocatalytic degradation of 2,4,6-tribromophenol over Fe-doped $ZnIn_2S_4$: Stable activity and enhanced debromination. *Appl. Catal. B Environ.*, 129: 89-97. doi:10.1016/j.apcatb.2012.09.007.

[15] Lee, H., Choi, J., Lee, S., Yun, S.T., Lee, C., Lee, J. (2013). Kinetic enhancement in photocatalytic oxidation of organic compounds by WO_3 in the presence of Fenton-like reagent. *Appl. Catal. B Environ.,* 138-139: 311-317. doi:10.1016/j.apcatb.2013.03.006.

[16] Gao, X., Su, X., Yang, C., Xiao, F., Wang, J., Cao, X., Wang, S., Zhang, L. (2013). Hydrothermal synthesis of WO_3 nanoplates as highly sensitive cyclohexene sensor and high-efficiency MB photocatalyst. *Sensors Actuators B Chem.*, 181: 537-543. doi:10.1016/j.snb.2013.02.031.

[17] Huo Y, Xie Z, Wang X, Li H, Hoang M, Caruso R.A (2013). Methyl orange removal by combined visible-light photocatalysis and membrane distillation. *Dye Pigment*, 98(1):106–12. doi:10.1016/j.dyepig.2013.02.009.

[18] Wang, J., Yu, Y., Zhang, L. (2013). Highly efficient photocatalytic removal of sodium pentachlorophenate with Bi_3O_4Br under visible light. *Appl. Catal. B Environ.* 136-137: 112–121. doi:10.1016/j.apcatb.2013.02.009.

[19] Miao, Z., Tao, S., Wang, Y., Yu, Y., Meng, C., An, Y. (2013). Hierarchically porous silica as an efficient catalyst carrier for high performance vis-light assisted Fenton degradation. *Microporous Mesoporous Mater.*, 176: 178-185. doi:10.1016/j.micromeso.2013.04.009.

[20] Zhang, Y., Wang, D., Zhang, G. (2011). Photocatalytic degradation of organic contaminants by TiO₂/sepiolite composites prepared at low temperature. *Chem. Eng. J.*, 173(1): 1-10. doi:10.1016/j.cej.2010.11.028.

[21] Gupta, V.K., Pathania, D., Agarwal, S., Singh, P. (2012). Adsorptional photocatalytic degradation of methylene blue onto pectin-CuS nanocomposite under solar light. *J. Hazard. Mater.*, 243: 179-186. doi:10.1016/j.jhazmat.2012.10.018.

[22] Xiao, X., Hu, R., Liu, C., Xing, C., Zuo, X., Nan, J., Wang, L. (2013). Facile microwave synthesis of novel hierarchical Bi₂₄O₃₁Br₁₀ nanoflakes with excellent visible light photocatalytic performance for the degradation of tetracycline hydrochloride. *Chem. Eng. J.*, 225: 790-797. doi:10.1016/j.cej.2013.03.103.

[23] Lu, S.Y., Wu, D., Wang, Q. L., Yan, J., Buekens, A.G., Cen, K.F. (2011). Photocatalytic decomposition on nano-TiO₂: Destruction of chloroaromatic compounds. *Chemosphere*, 82 (9):1215-1224. doi:10.1016/j.chemosphere.2010.12.034.

[24] Mahmoodi, N.M., Arami, M., Limaee, N.Y (2006). Photocatalytic degradation of triazinic ring-containing azo dye (Reactive Red 198) by using immobilized TiO₂ photoreactor: Bench scale study. *J. Hazard. Mater.*, 133(1-3): 113-118. doi:10.1016/j.jhazmat.2005.09.057.

[25] Mu, R., Xu, Z., Li, L., Shao, Y., Wan, H., Zheng, S. (2010). On the photocatalytic properties of elongated TiO₂ nanoparticles for phenol degradation and Cr(VI) reduction. *J. Hazard. Mater.*,176 (1-3): 495–502. doi:10.1016/j.jhazmat.2009.11.057.

[26] Yang, S., Gu, J.S., Yu, H.Y., Zhou, J., Li, S.F., Wu, X.M., Wang, L. (2011). Polypropylene membrane surface modification by RAFT grafting polymerization and TiO₂ photocatalysts immobilization for phenol decomposition in a photocatalytic membrane reactor. *Sep. Purif. Technol.* 83: 157-165. doi:10.1016/j.seppur.2011.09.030.

[27] Wang, N., Chu, W., Zhang, T., Zhao, X. (2011). Manganese promoting effects on the Co–Ce–Zr–Ox nano catalysts for methane dry reforming with carbon dioxide to hydrogen and carbon monoxide. *Chem. Eng. J.*, 170(2-3): 457-463. doi:10.1016/j.cej.2010.12.042.

[28] Gupta, V.K. (2009). Application of low-cost adsorbents for dye removal - A review. *J. Environ. Manage.*, 90 (8): 2313-2342. doi:10.1016/j.jenvman.2008.11.017.

[29] Meriläinen, A., Seppälä, A., Kauranen, P. (2012). Minimizing specific energy consumption of oxygen enrichment in polymeric hollow fiber membrane modules. *Applied energy*, 94: 285–294. doi:10.1016/j.apenergy.2012.01.069.

[30] Peng, N., Widjojo, N., Sukitpaneenit, P., Teoh, M.M., Lipscomb, G.G., Chung, T.S., Lai, J.Y. (2012). Evolution of polymeric hollow fibers as sustainable technologies: Past, present, and future. *Prog. Polym. Sci.*, 37 (10): 1401-1424. doi:10.1016/j.progpolymsci.2012.01.001.

[31] Luttrell, T., Halpegamage, S., Tao, J., Kramer, A., Sutter, E., Batzill, M. (2014). Why is anatase a better photocatalyst than rutile?- Model studies on epitaxial TiO₂ films. *Scientific Reports*, 4: 4043.

[32] Li, X., Xiong, Y., Zou, L., Wang, M., Xie, Y. (2007). Polymer-induced generation of anatase TiO₂ hollow nanostructures. *Microporous and Mesoporous Materials* 112 (1-3): 641–646. doi:10.1016/j.micromeso.2007.10.034.

[33] Benedix, R., Dehn, F., Quaas, J., Orgass, M. (2000). Application of titanium dioxide photocatalysis to create self-cleaning building materials. *Lacer*, 3: 157-168.

[34] Damodar, R.A., You, S., Chou, H. (2009). Study the self cleaning , antibacterial and photocatalytic properties of TiO₂ entrapped PVDF membranes. *Journal of Hazardous Materials*, 172(1-3): 1321-1328. doi:10.1016/j.jhazmat.2009.07.139.

[35] Dzinun, H., Othman, M.H.D., Ismail, A.F., Puteh, M.H., Rahman, M.A., Jaafar, J. (2016). Photocatalytic degradation of nonylphenol using co-extruded dual-layer hollow fibre membranes incorporated with a different ratio of TiO₂/PVDF. *React. Funct. Polym.*, 99: 80-87. doi:10.1016/j.reactfunctpolym.2015.12.011.

[36] Liang, S., Kang, Y., Tiraferri, A., Giannelis, E.P., Huang, X., Elimelech, M. (2013). Highly Hydrophilic Polyvinylidene Fluoride (PVDF) Ultrafiltration Membranes via Postfabrication Grafting of Surface-Tailored Silica Nanoparticles. *ACS Appl. Mater. Interfaces*, 5 (14): 6694-6703. doi:10.1021/am401462e.

[37] Akpan, U.G., Hameed, B.H. (2009). Parameters affecting the photocatalytic degradation of dyes using TiO₂-based photocatalysts : A review. *Journal of Hazardous Materials*, 170(2-3): 520-529. doi:10.1016/j.jhazmat.2009.05.039.

[38] Kang, G.D., Cao, Y. (2014). Application and modification of poly(vinylidene fluoride) (PVDF) membranes - A review. *J. Memb. Sci.*, 463:145-165. doi:10.1016/j.memsci.2014.03.055.

[39] Liu, F., Hashim, N.A., Liu, Y., Abed, M.R.M., Li, K. (2011). Progress in the production and modification of PVDF membranes. *J. Memb. Sci.*, 375(1-2): 1-27. doi:10.1016/j.memsci.2011.03.014.

[40] Ngang, H.P., Ooi, B.S., Ahmad, A.L., Lai, S.O. (2012). Preparation of PVDF-TiO₂ mixed-matrix membrane and its evaluation on dye adsorption and UV-cleaning properties. *Chem. Eng. J.*, 197: 359-367. doi:10.1016/j.cej.2012.05.050.

[41] Houas, A., Lachheb, H., Ksibi, M., Elaloui, E., Guillard, C., Herrmann, J.M. (2001). Photo-catalytic degradation pathway of methylene blue in water. *Appl. Catal. B* Environ., 31 (2): 145-157. doi:10.1016/S0926-3373(00)00276-9.

[42] Konstantinou, I.K., Albanis, T.A. (2004). TiO₂-assisted photocatalytic degradation of azo dyes in aqueous solution: Kinetic and mechanistic investigations: A review. *Appl. Catal. B Environ.*, 49 (1): 1-14. doi:10.1016/j.apcatb.2003.11.010.